SSRG International Journal of Electrical and Electronics Engineering
ISSN: 2348-8379/ https://doi.org/10.14445/23488379/IJEEE-V11I4P120

Volume 11 Issue 4, 184-197, April 2024

Original Article

Design of a Wideband Moon-Shaped Microstrip Patch Antenna for Wearable Applications in Cellular Communication

Chetan Sambhajirao More[1], Navnath Tatyaba Markad[2]

[1,2]*Bharati Vidyapeeth (Deemed to be University) College of Engineering, Pune, India.*

[1]*Corresponding Author : csmore@bvucoep.edu.in*

Received: 12 February 2024 Revised: 13 March 2024 Accepted: 12 April 2024 Published: 30 April 2024

Abstract *- This paper introduces the development of a novel moon-shaped microstrip antenna featuring a Defected Ground Structure (DGS) optimized for wearable technology applications. Aimed at addressing the critical need for compact yet efficient wireless communication solutions in wearable devices, this antenna design emphasizes a blend of aesthetic conformity and functional robustness. The proposed antenna, characterized by dimensions of a 34.04 mm width and a 40 mm height, operates across a broad frequency range with a resonant frequency cantered around 3.29 GHz; this makes it suitable for multiple wireless protocols, including Wi-Fi and Bluetooth. Employing a Coplanar Waveguide (CPW) feed technique, the design achieves an enhanced bandwidth and superior impedance matching, evidenced by a reflection coefficient of -19.3 dB at the resonant frequency. The antenna operates optimally across a multi-frequency band, exhibiting significant promise at the 3.29 GHz frequency, making it well-suited for various communication standards, including but not limited to Wi-Fi, Bluetooth, and potential 5G applications. Simulation and experimental results underscore its robust performance in terms of impedance matching, showcasing a VSWR less than 2:1 and an impressive reflection coefficient (S11) value across the operational bandwidth.*

Keywords *- Moon-shaped microstrip antenna, Wearable device, Defected Ground Structure (DGS), Coplanar Waveguide (CPW), Multi-frequency band operation.*

1. Introduction

In the rapidly evolving realm of wearable technologies, the integration of efficient and compact antennas is paramount to ensuring seamless wireless communication. Traditional microstrip antennas, with their simplicity and ease of manufacturing, often fall short in terms of bandwidth and compactness, especially for lower frequencies. Addressing these challenges, to address existing design challenges, an innovative approach has been developed for a thin-film microstrip antenna. This approach incorporates a moon-shaped geometry and a defected ground structure, which collectively enhance the antenna's operational bandwidth and maintain its low profile [1, 2].

This novel design not only meets the stringent requirements of modern communication systems but also aligns with the aesthetic and functional needs of wearable devices. By strategically modifying the ground plane and the radiating element, our approach improves impedance matching over a wider bandwidth, which is crucial for the diverse frequencies employed in consumer electronics, medical monitoring, and personal communication. The proposed antenna's unique structure not only optimizes current distribution for better performance but also ensures it remains unobtrusive and flexible for integration into everyday wearables [3]. This advancement marks a significant step forward in the development of antennas that are not only performance-driven but also user-friendly, opening new avenues for the next generation of wearable technology.

In the domain of wireless communications, the ISM band stands as a pivotal spectrum, encompassing frequencies from 2.4 GHz to 2.485 GHz, predominantly utilized for Wi-Fi along with Bluetooth and microwave oven applications. This band is characterized by its global, unlicensed accessibility, albeit with specific regulatory limitations that vary by jurisdiction. Wi-Fi technology, leveraging this band, primarily operates across the 2.4 GHz and 5 GHz frequencies. Governed by the IEEE 802.11 series, Wi-Fi encompasses a suite of protocols designed to meet diverse requirements in terms of speed and operational range [4-6].

Simultaneously, Mobile WiMAX emerges as a key player in broadband wireless access, spanning several operational

bands, including 2.30-2.40 GHz, 2.50-2.70 GHz, 3.40-3.70 GHz and 4.90-5.40 GHz. Rooted in the IEEE 802.16 standard, WiMAX is engineered to deliver broadband coverage across vast areas, facilitating a myriad of uses from internet provisioning to cellular backhaul. The technology is underpinned by standards like IEEE 802.16a, focusing on fixed broadband within the 10-16 GHz range, and IEEE 802.16-2004, or 802.16d, which caters to fixed applications across the 2-11 GHz spectrum. Integral to both Wi-Fi and WiMAX, OFDM and OFDMA represent cornerstone modulation and access methods, respectively. These technologies are instrumental in optimizing spectrum utilization, ensuring high-speed, reliable wireless connectivity across an array of networks [7, 8].

In recent years, the integration of textile materials into antenna design has emerged as a significant area of research, particularly for enhancing wearable technology communication capabilities within the ISM band, notably at the 2.45 GHz frequency. This focus is driven by the frequency's widespread use in wireless communication technologies like Wi-Fi and Bluetooth, offering a blend of global accessibility and compatibility with a vast array of devices. The innovative approach to incorporating textiles into antenna designs marks a pivotal shift towards creating more user-friendly and functional wearable tech [5-9].

A groundbreaking study by Bhaldar and colleagues in 2020 unveiled a microstrip textile antenna tailored for Wi-Fi communication that operates effectively at 2.45 GHz. This antenna distinguishes itself through its use of denim as a dielectric substrate, showcasing a return loss measured at -15.760 dB and directivity reaching 8.050. The antenna excels in minimizing signal reflections and focusing energy effectively, achieved with its rectangular configuration. This research underscores the potential of common materials like jeans to provide substantial bandwidth and effective electromagnetic performance, hinting at the practical applications of wearable tech in daily life [9].

Further exploration into wearable antennas was conducted by Carlos et al. in 2018, who introduced an on-body antenna and a robust snap-on button design, both optimized for the 2.45 GHz ISM band. These designs demonstrated return losses of -18 dB and -25 dB, respectively, illustrating the feasibility of seamlessly integrating antenna technology into clothing for enhanced wireless communication [10, 11].

In a similar vein, Pranita Manish and her team in 2018 conducted a comparative analysis of microstrip textile antennas utilizing various fabric materials as dielectric substrates, including Cotton, Polyester, Cordura, and Lycra. Their findings revealed significant variations in return loss performance across these materials at the 2.45 GHz frequency, highlighting the critical role material selection plays in optimizing antenna functionality for wearable applications [12]. Safety considerations, particularly regarding the Specific Absorption Rate (SAR), have also been paramount in the development of wearable antennas. Sweety Purohit and colleagues 2014 emphasized the importance of maintaining SAR values within safe limits, demonstrating through their research with jeans material antennas that it's possible to achieve both effective communication and adherence to health standards in wearable technology [13].

Expanding the scope of antenna design, Jiahao Zhang et al. 2017 delved into the development of a miniature feeding network for aperture-coupled antennas, operating within the 2.4 GHz to 2.483 GHz range. Their investigation into various aperture shapes, including rings and E-shapes, contributed to a better understanding of how physical configurations can enhance antenna gain and performance across the ISM band [14]. The wearable fractal antenna working at 2.53GHz, 4.9GHz, and 7.6GHz for S, C, and X band applications was investigated and analyzed by Sandeep Singh Sran et al. in 2020. At these resonance frequencies, the gain and bandwidth of the suggested antenna were increased [15, 16].

The literature review guided the proposed antenna design towards augmenting gain and bandwidth. Tailored for wearable devices, the antenna employs a defective ground structure to expand bandwidth while maintaining a compact size. The design adeptly balances the conventional trade-off between size and bandwidth, catering to various wireless protocols. A coplanar waveguide feed boosts impedance matching, a feature substantiated by simulation and empirical tests. This advancement in antenna design integrates high performance with the practicality required for wearable technology.

1.1. Suitable Applications for Proposed Antenna

Given the observed bandwidth and the resonant frequency around 4 GHz, this antenna could be suitable for several applications:

- Wi-Fi Connectivity: The resonant frequency is close to the 5 GHz band used for Wi-Fi, which means the antenna could be used for wearable devices requiring high-speed data connectivity. The 3.6 GHz band is within the range used by Wi-Fi (IEEE 802.11), which can be beneficial for wearable devices that require connectivity to local area networks for data communication.
- Industrial, Scientific, and Medical (ISM) Band Applications: The ISM bands around 2.40 and 5.80 GHz are widely used for medical devices, Bluetooth, and other wireless communication systems that could benefit from the antenna's bandwidth. Wearable medical devices that require data transmission within a healthcare facility might operate within this band to communicate with central monitoring systems [8].
- Positioning and Location Tracking: The antenna could be used in devices for indoor navigation or activity tracking,

where compact size and integration into clothing or accessories are beneficial.

- Wearable Technology: Devices like smartwatches, fitness trackers, and medical monitoring equipment could utilize this antenna design for its compact size and reliable performance in the required frequency bands.
- UWB Applications: If the bandwidth is sufficiently wide, it may cover part of the ultra-wideband (UWB) spectrum, which is used for high-bandwidth applications requiring precise location tracking and data transmission [17].

2. Design of Moon-Shaped Microstrip Patch Antenna

The proposed antenna design, as depicted in the accompanying schematic, features a moon-shaped radiating patch which optimizes the trade-off between size and performance. The defected ground structure (DGS) technique has been applied to introduce a band gap characteristic, effectively increasing the operational bandwidth without increasing the physical dimensions of the antenna [17, 18]. This antenna layout strategically places the ground plane and radiating patch on the same plane, ensuring they are not positioned too closely to prevent signal degradation and enhance effectiveness.

This arrangement simplifies the fabrication process, especially for thin-film applications. The feed line is carefully designed to match the 50-ohm impedance, ensuring maximum power transfer [19]. The defective ground structure creates a patterned defect in the ground plane, contributing to a wider operational bandwidth. The DGS technique is known to increase the current path length, thereby lowering the resonant frequency for a given total dimension of the antenna. The design incorporates a simulated Sub Miniature version (SMA) connector for feeding the antenna, depicted as the black part at the bottom centre of the design. The SMA connector is widely used due to its robustness and frequency performance, making it suitable for wearable applications that require durability and reliability [19-23].

2.1. Antenna Schematic Analysis

- The antenna is designed for a frequency sweep from 1 to 6 GHz, with a step size of 100 MHz. This wide range suggests that the antenna could be used for multiple applications across the spectrum, from UHF to C band.
- A dielectric constant of 4.4 is moderately high, which reduces the wavelength of the signal within the substrate, allowing for a smaller antenna design than if a lower dielectric constant material were used.
- Feed Line: The central vertical line in the design represents the feed line, which links to the patch. While its exact width isn't specified, it appears to be roughly a few millimeters wide, judging from the scale provided.
- Substrate: The grey areas around the patch represent the dielectric substrate on which the patch is mounted. The dielectric constant of this substrate is given as 4.4, which affects the antenna's impedance and radiation properties.
- Ground Plane: The size of this ground plane is essential because it significantly impacts the antenna's bandwidth and the pattern of radiation emitted, which are critical factors for its overall performance.
- Parameter Sweeping involves varying design parameters within certain ranges and observing the effect on S11 and Zin.

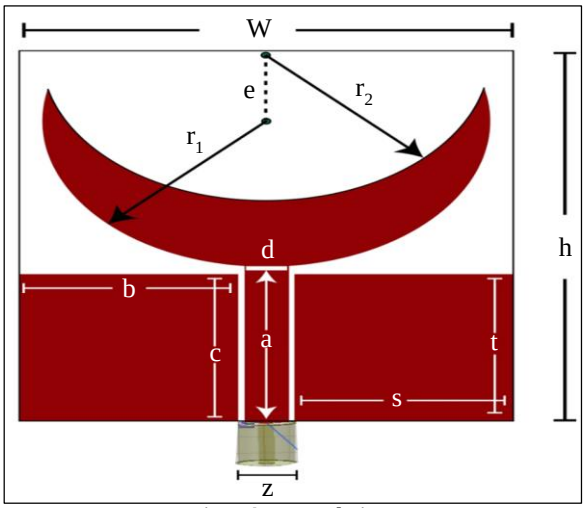

Fig. 1 Antenna design

This antenna is a small, flat radio device that can be placed on clothing or skin for wireless communication. The crescent shape helps it to fit into a compact space and potentially gives it unique characteristics for sending and receiving signals. It's designed to be thin and unobtrusive, which is why it might be described as a 'thin-film' antenna [24]. This common substrate material used is copper, with a dielectric constant typically around 4.4, which impacts the antenna's performance and dimensions.

- Width (W) and Height (h): These are the dimensions of the rectangular piece of material (substrate) that supports the antenna. It's like the foundation that the circular patch sits on.
- Patch Radius (r1 and r2): These numbers tell us how big the circular part of the antenna is. Since both r1 and r2 are the same (15 mm), this means the diameter of the full circle is 30 mm.
- Feed Width and Length (p, s, q, t): The feed is the part that connects to the rest of the circuit, bringing in the signal that the antenna will transmit or receive. It has a specific width and length (both 15 mm and 16 mm, respectively) that helps the antenna work at the correct frequency.
- Substrate Dimensions (a and d): The measurements labeled as 'a' and 'd' in the diagram likely indicate the substrate's thickness and the width of a specific part of either the feed, respectively.

- SMA Connector Position (z): This is where the connector is placed, which is how the antenna connects to other devices. It's a small distance from the bottom edge (4 mm).
- Off-center Distance (e): This is a key dimension that shows the circular patch is not in the middle of the substrate but is moved to one side by 7.3 mm.

The antenna's performance, including the frequencies it can operate at and the efficiency with which it can send or receive signals, is largely dependent on the dimensions of its component parts. To put it another way, consider the antenna as a particular form of radio wave "speaker"; to "play" the waves at the proper pitch (frequency), the patch and substrate of the speaker must be precisely the right size and shape.

- Resonant Frequency (f_0) :

$$f_0 = \frac{c}{2\pi R_{\text{eff}}\sqrt{\epsilon_{\text{eff}}}}$$

- Effective Dielectric Constant $(\varepsilon_{\text{eff}})$:

$$\epsilon_{\text{eff}} = \frac{\epsilon_r + 1}{2} + \frac{\epsilon_r - 1}{2}\left(1 + 12\frac{h}{D}\right)^{-1/2}$$

- $\epsilon_{\text{eff}} = \frac{t+1}{2} + \frac{1}{2}\left(1 + 12\frac{h}{W}\right)^{-1/2}$ - Extended length due to fringing (ΔL).

$$\Delta L = 0.412h\left(\frac{\epsilon_{\text{r}//} + 0.3}{\epsilon_{\text{m}/J} - 0.258}\right)\left(\frac{W}{h + 0.264}\right)$$

Patch Length Calculation

- Actual Length (L) :

$$L = \frac{c}{2f+\sqrt{3\pi/L/}} - 2\Delta L$$

- Width (W) of the patch

$$W = \frac{c}{2f\sqrt{\varepsilon_{nefs}}} = \frac{c}{2f_r\sqrt{t_r}}$$

- Extended Radius (R_{eff}) considering fringing effect:

$$R_{eff} = R + \Delta R$$

- Return Loss

Return loss, which indicates how well the antenna matches its load, can be calculated if the reflection coefficient S_{11} is known through:

$$\text{Return Loss} = -20\log_{10}(|S_{11}|)$$

Where:

- c is the speed of light in a vacuum $(3 \times 10^8\ \text{m/s})$,
- R is the radius of the patch,
- D is the diameter of the patch
- h is the height of the substrate, 40mm
- $\epsilon_r = 4.4\ (For\ FR4)$ is a relative permittivity of the substrate
- ϵ_{eff} is an effective dielectric constant

Table 1. Antenna dimension

Sl. No.	Parameter	Dimensions (mm)
1	Width (W)	34.04
2	Height (h)	40
3	Patch Radius (r1)	15
4	Patch Radius (r2)	15
5	Distance from the centre of the circular patch to the line of symmetry of the substrate (e)	7.3
6	Feed Width (p and s)	15
7	Feed Length (q and t)	16
8	Substrate Height (a)	17
9	Substrate Width (d)	3.2
10	SMA Connector Position (z)	4
11	Substrate Material	4.4 (FR4)
12	Patch and Ground Material	Copper
13	Feeding Technique	Coplanar Waveguide Feed (CPW)
14	Defected Ground Structure	Yes

The antenna uses a Coplanar Waveguide Feed (CPW), which helps achieve superior impedance matching. This feed technique is beneficial for thin-film applications due to its simplicity and effectiveness in maintaining a compact and flexible design.

Possible Influencing External Factors on Antenna: Given the complexity of designing antennas like the moon-shaped microstrip patch antenna, especially for wearable applications, it's essential to consider external factors that could influence their performance.

Wearable Technology Constraints: The antenna's design must consider the interaction with the human body, which can affect the antenna's performance due to the absorption of radio waves by body tissues.

Environmental Factors: Factors like humidity, temperature, and physical obstructions can affect the antenna's performance, especially in wearable applications.

Material Flexibility and Durability: Since the antenna is designed for wearable applications, the materials used need to be flexible and durable enough to withstand various environmental stresses without degrading the antenna's performance.

For Example, Let's consider the impact of body proximity on the return loss of the antenna using a simplified model. Designed for a 3.5 GHz operation in free space, the antenna may experience a frequency shift when placed in proximity to the human body. This is due to the body's muscle tissue having a relative permittivity near 50, which can elevate the effective dielectric constant and detune the antenna from its planned resonant frequency.

$$\text{Effective Dielectric Constant } (\epsilon_{eff}) = \frac{\epsilon_{r,\text{ air}} + \epsilon_{r,\text{ body}}}{2}$$

Where $\epsilon_{r,air} = 1$ (free space), $\epsilon_{r,body} = 50$ (an approximation for muscle).

$$\epsilon_{\text{eff}} = \frac{1+50}{2} = 25.5$$

- Increased ϵ_{eff} leads to a lower resonant frequency than designed.
- Implementing a High-Impedance Surface (HIS) or using materials with a controlled dielectric constant can help in maintaining the desired resonant frequency.

3. Simulation and Results Moon-Shaped Microstrip Antenna

Begin by detailing the simulation software used by Ansys HFSS, including the version and any relevant settings or assumptions made within the model. Here, the boundary conditions and the mesh grid are applied to solve Maxwell's equations for this particular antenna design. Using high-fidelity electromagnetic simulation tools, the proposed antenna focuses on the reflection coefficient (S11) and VSWR [27]. The black element at the bottom centre of the design represents the SMA connector used to feed the signal into the antenna, ensuring a practical connection for real-world applications [26].

The reflection coefficient's role in antenna design is crucial as it indicates the power reflection back into the system, with lower values near 0 dB suggesting better impedance matching. Figure 2 demonstrates this with a significant dip in the reflection coefficient around 3.3 GHz, where the antenna achieves optimal matching with the transmission line, dipping below -10 dB, a threshold indicating a substantial reduction in reflected power.

This resonant frequency allows the antenna to perform well, particularly noted by a reflection coefficient of -19.3 dB at 3.29 GHz. The antenna's operational bandwidth, indicated by the range over which the reflection coefficient stays under -10 dB, suggests effective performance across a spectrum extending from 2.75 GHz to 4.86 GHz, beneficial for diverse wearable device applications.

Figure 3 shows reflection; the graph starts with extremely high VSWR values at low frequencies, indicating poor impedance matching and, therefore, significant power reflection. The plot then levels off, which suggests that an optimal match has been reached and maintained over a certain frequency range. As the frequency increases, the VSWR rapidly decreases and flattens out, suggesting improved impedance matching. Ideally, VSWR is close to 1 across the operating frequency band for the best performance. The antenna's best match to the transmission line occurs when the VSWR reaches its lowest point. The flat part of the curve at the bottom indicates the frequency range where the antenna maintains a good match.

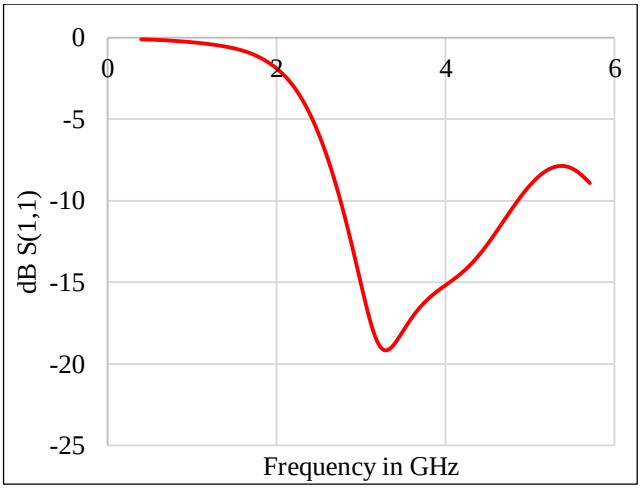

Fig. 2 Reflection coefficient

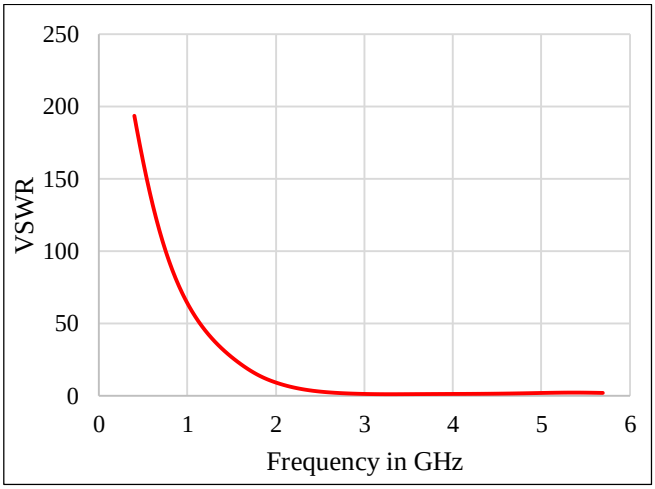

Fig. 3 VSWR

VSWR of 1:1 means a perfect match; as the number increases, the match worsens, indicating more power is reflected back towards the source [17], but in purposed antenna, VSWR is below certain thresholds (such as 2:1 or 1.5:1) to define the antenna's operational bandwidth. For wearable applications, this bandwidth should align with the frequencies used by the devices the antenna is meant to communicate with. A low and stable VSWR is crucial for ensuring that the antenna efficiently radiates the energy, which is particularly important in power-sensitive applications like wearable technology.

In Figure 4, the 3D radiation pattern plots are indicative of the spatial characteristics of an antenna's radiated electromagnetic fields at the specified operational frequencies of 2.75 GHz, 3.29 GHz, and 4.86 GHz. These plots are essential for determining the directional emission and reception capabilities of the antenna.

The scale or color gradation represents the magnitude of the radiated field, quantified in terms of electric field strength (V/m) or power density (dB). In these plots, the color gradation, which transitions from cool to warm colors, represents the relative magnitude of the radiated field. The regions depicted in red signify the areas of strongest radiation, also referred to as the main lobe or the peak radiation direction. These are critical for identifying the antenna's maximum gain, which is a measure of the power concentration in a particular direction compared to an isotropic source. The θ (theta) and ϕ (phi) angles delineate the radiation direction with respect to the antenna. θ is the angle from the zenith (the point directly above the antenna), ranging from 0° (upwards) to 180° (downwards). ϕ is the azimuthal angle in the horizontal plane starting from a reference direction, like north.

Directivity quantifies how energy is focused in a specific direction, with higher directivity beneficial for targeted communications. Operating frequency is crucial, as antennas are optimized for specific frequency bands tailored to their application (e.g., cellular, GPS, Wi-Fi).

Beamwidth, the spread of the main radiation lobe, influences coverage area and is key in antenna array design for ensuring proper pattern overlap. For wearable technology, antenna design must balance compactness with safety, favoring omnidirectional patterns to maintain consistent communication while minimizing radiation exposure to the wearer for health compliance.

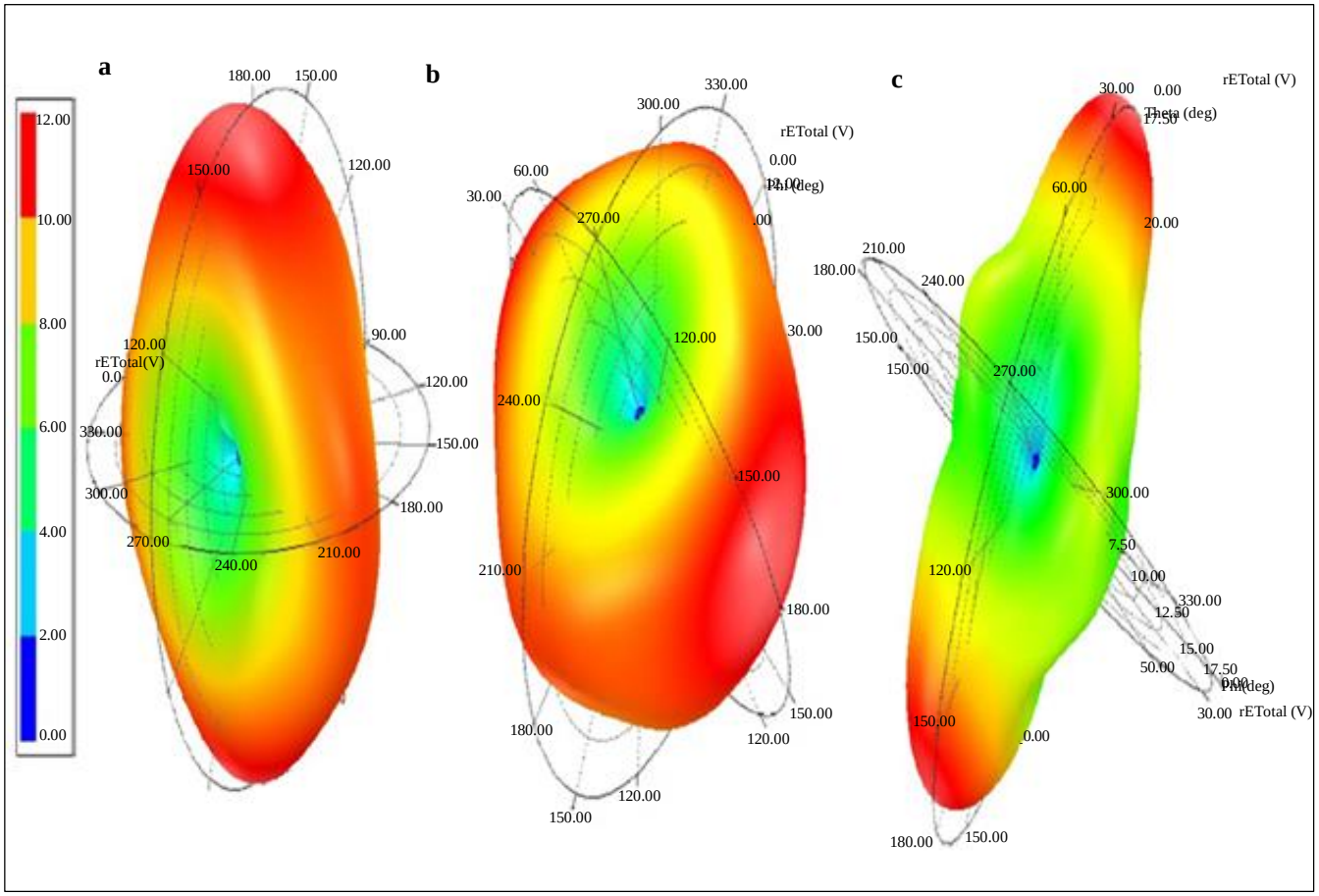

Fig. 4 3D Radiation pattern (a) 2.75 GHz, (b) 3.29 GHz, and (c) 4.86 GHz.

Table 2. Observation of radiation pattern at (a) 2.75 GHz, (b) 3.29 GHz, and (c) 4.86 GHz.

Frequency (GHz)	Peak Gain (dBi)	3dB Beam Width (degrees)	Front-to-Back Ratio (dB)	Side Lobe Level (dB)	Main Lobe Magnitude	Beam Width	Side Lobe Level	Remarks
2.75	12.5	70	25	-18	High (Red)	Wide	Moderate (Green/ Yellow)	Broad Coverage, Less Directional
3.29	12.5	65	28	~20	Very High (Bright Red)	Narrow	Low (Blue/Green)	Focused Beam, Higher Directivity, Lower Sidelobe Levels
4.86	14	60	30	~25	Moderate (Yellow/ Orange)	Moderate	High (Yellow/Red)	Wider Beam than 3.29 GHz, More Sidelobe Activity than 3.29 GHz

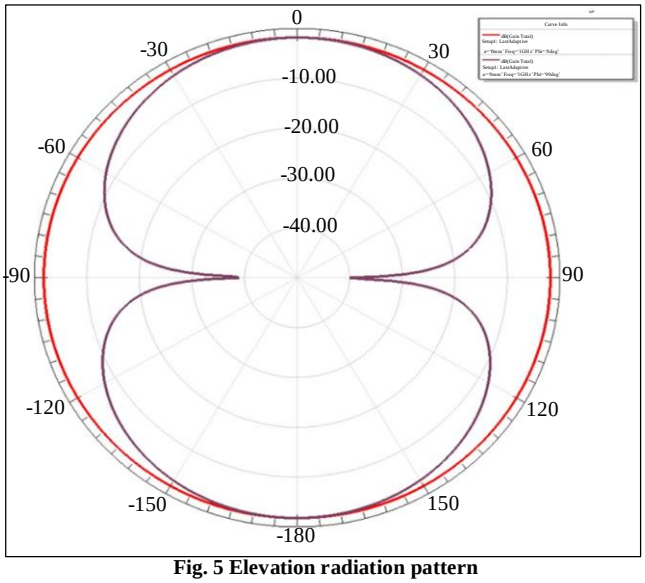

Fig. 5 Elevation radiation pattern

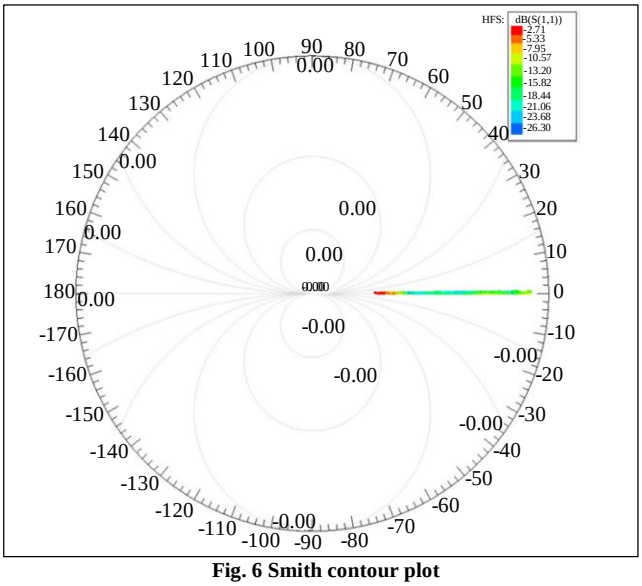

Fig. 6 Smith contour plot

Figure 5 illustrates an antenna's elevation radiation pattern through a polar plot, which effectively demonstrates the distribution of radiated energy by the antenna at varying elevations. Taken from a vertical plane within the antenna's three-dimensional radiation pattern, this 2D slice shows detailed azimuth cuts at Phi=0deg and Phi=90deg. The plot highlights the main lobe extending along the 0-degree elevation, the prime direction of maximum gain, signifying the antenna's optimal radiation efficiency.

Additionally, the plot details the beamwidth of the antenna at the -3 dB points, which indicates the focus or spread of the radiated energy, essential for determining suitable applications based on directional needs. The elevation radiation pattern shows a Figure 6 distribution, indicative of a dipole-like radiation pattern. This reveals the antenna's directivity in the vertical plane, which has significant implications for the antenna's elevation beam width and gain. The lobes indicate the directions where the antenna radiates most efficiently and are symmetrical about the horizon.

Figure 6 shows the Smith Contour Plot; contour lines indicate constant values of reflection coefficient magnitude, which are labelled in decibels (dB). This is a visualization in the form of a polar plot that captures the complex reflection coefficient (Γ), highlighting its values in a rotational symmetry.

The outer circle represents points where the reflection coefficient has a magnitude of 1 (total reflection), and the center of the chart (the origin) represents points where the reflection coefficient has a magnitude of 0 (total transmission, no reflection). The horizontal line near the center might indicate a sweep of the frequency with a mostly resistive load since it remains close to the horizontal axis, which is the real axis in the Smith chart.

The green area extending to the red at the right side indicates a range where the reflection coefficient is lowest and where the antenna or transmission line is best matched to the load.

- Red: Highest reflection (around -2.71 dB)
- Yellow to Green: Gradually lower reflection
- Green: Lowest reflection measured in this plot (around -26.30 dB)

The colors along the plotted line likely represent the magnitude of the reflection coefficient ($|S_{11}|$) at different frequencies, with the key provided in dB. From the set of scattering parameters, S_{11} specifically represents the fraction of power that is returned to the originating source by the antenna or load. High gain in a particular direction indicates a focused beam, which is useful for long-range communication. In contrast, a more uniform distribution of gain would be indicative of an omnidirectional antenna.

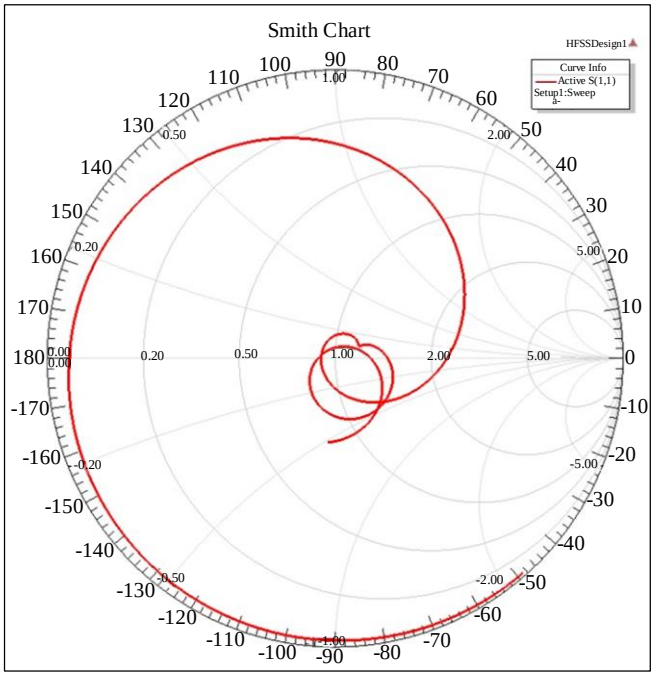

Fig. 7 Smith chart

In Figure 7, the centre of the Smith chart represents a normalized impedance (or admittance) of 1+j0, which corresponds to A transmission line's characteristic impedance, is crucial for matching the line to its load to ensure efficient signal transmission without reflections, typically 50 ohms. The outer edge of the chart represents infinite impedance or zero impedance points (short or open circuits).

The circles that run around the centre represent constant reflection coefficient magnitudes (constant SWR levels), and the radial lines represent constant phases of the reflection coefficient. Reflection Coefficient: The distance from the centre point to the plotted curve gives the magnitude of the reflection coefficient. A smaller distance indicates a better match. The chart is used for impedance matching by providing a visual tool to adjust the impedance of the line or antenna system to minimize reflections and standing waves.

The constant SWR (Standing Wave Ratio) circles help determine how close the system is to an ideal match. The intersection of the curve with these circles provides the SWR value. The red curve on the Smith chart represents a locus of points that characterize the impedance or admittance variations over a range of frequencies, lengths of transmission lines, or other parameters.

The curve appears to start from the right edge, around the purely resistive axis (indicated by the normalized resistance value of 1.00), suggesting the system starts with an impedance close to the characteristic impedance of the transmission line (normalized to 1.00). The spiral inward indicates a change in impedance, possibly due to the length of the transmission line or a frequency sweep. As the spiral moves inwards and clockwise, it demonstrates a varying impedance that is initially inductive (above the center line) and then becomes capacitive (below the center line).

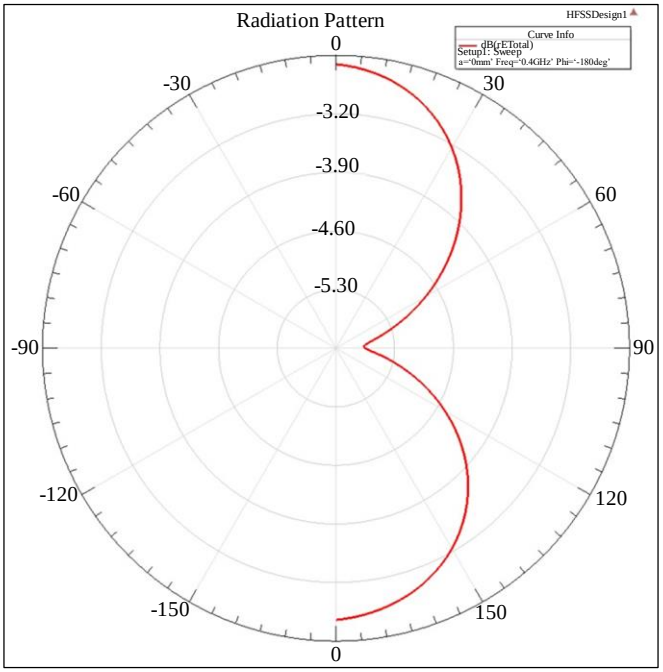

Fig. 8 Radiation pattern

In Figure 8, the plot shows a spiraling inward pattern starting close to the outer edge of the chart and moving towards the center. This indicates that the parameter it represents is changing significantly over the sweep. The information on the chart indicates a frequency of 0.4 GHz (400 MHz) and a Phi (likely the azimuth angle) of -180 degrees. The 'a=0mm' might suggest the radial distance from the center of the system or a reference point within the antenna design is 0 mm, implying that this may be a parameter sweep at the phase center of the antenna; the chart may be representing the normalized radiation pattern or gain at a constant frequency of 0.4 GHz as the antenna is rotated, which is often done in antenna measurements.

Table 3. Analysis of simulation results for a moon-shaped microstrip antenna's performance

Parameter	Smith Chart	Radiation Pattern	Directivity Chart	Smith Contour Plot
Purpose	Impedance Matching	Power Distribution	Directivity Analysis	Reflection Coefficient Analysis
Typical Usage	Designing matching Networks	Analyzing Antenna Radiation Properties	Determining how Focused the Radiation is	Checking Impedance Mismatches
Key Observable	Reflection Coefficient (Γ)	Radiation Intensity (U)	Directivity (D)	Return Loss
Variable Against	Position along the Transmission Line or Frequency	Angle in space	Angle in Space	Frequency or Varying Load
Measurable Parameters	VSWR, Impedance (Z)	Gain (G), Beamwidth, Sidelobes	Peak Directivity, Beam Efficiency	S11 Magnitude and Phase
Performance Metrics	How Well the Antenna is Matched To the Transmission Line	How Effectively does the Antenna Radiate Power	How Directional the Antenna is	How much Power is Reflected Back to the Source
Design Considerations	The Closer to the Center, the Better the Match	Desired Radiation Pattern Shape for Application	Achieve the Highest Directivity in the Desired Direction	Minimize Reflection for Maximum Power Transfer
Primary Use	Matching Network Analysis	Analyzing Radiation Characteristics	Antenna Directivity Analysis	Evaluating Impedance Matching

4. Experimental Verification

The experimental analysis involves fabricating the proposed antenna, as depicted in Figure 12, which shows a moon-shaped microstrip patch antenna on jeans cloth. The metal patch is affixed over a larger metal ground plane. A microstrip line feed supplies RF energy to the patch, and it is essential to match the impedance of the feed line with the antenna's impedance to reduce reflections and maximize power transfer. The SMA connector is where the antenna connects to the rest of the RF system. A proper connection ensures the RF signal is delivered efficiently to and from the antenna. The radius of the moon-shaped patch microstrip antenna is calculated for the resonant frequency of 2.4GHz & dielectric constant for jeans is 1.7. By using equation [9],

$$f_{mn} = \frac{c}{2\pi a\sqrt{\varepsilon r}} x_{mn}$$

Where $c = \frac{1}{\sqrt{\mu_0 \varepsilon_0}}$ speed of light
F_{mn} = Resonating frequency for mn mode
a = Radius of patch
x_{mn} = Constant for mn mode
εr = Relative dielectric constant substrate

Table 1 shows the list of antenna parameters used to design circular microstrip antenna.

Figure 9 fetching a pattern Defected Ground Structure (DGS) Moon-Shaped Microstrip to improve its performance by disrupting the surface currents, potentially lowering cross-polarization and mutual coupling between elements in an array. The dielectric constant for jeans is 1.7 which is quite low, indicating that it's less dense than typical antenna substrates like FR4. This would result in a slower wave propagation speed and could lead to a larger wavelength for the same frequency, potentially requiring a larger antenna size for resonance at a given frequency compared to a higher permittivity substrate.

The CPW feed is a transmission line where the signal and ground conductors are on the same plane. It has advantages in terms of ease of manufacturing and is suitable for integration with planar circuits. CPW feed structures are often used for wideband antennas and facilitate easy integration with RF devices.

Fig. 9 Fabricated antenna

Using a CPW feed in this antenna means that the radiating element and the ground plane and the radiating element are located on the same side of the substrate, simplifying the feed structure and reducing the profile of the antenna. This type of feed is conducive to wearable applications due to its simplicity and compatibility with flexible substrates. The antenna is designed for wearable applications, which require antennas to be flexible, low-profile, durable, and have minimal interaction with the human body. The 5G communication aspect indicates that the antenna is meant to operate in the frequency bands allocated for 5G. The bandwidth of the antenna is critical for 5G applications, which require wide bandwidth to support high data rates. This can be estimated by measuring the VSWR or return loss around the resonant frequency and identifying the frequency range over which the VSWR is less than 2:1, or the return loss is below -10 dB. Such antennas are widely used in wireless communication systems, including mobile devices, satellite communication, and radar systems, due to their compatibility with printed circuit technology and ease of fabrication.

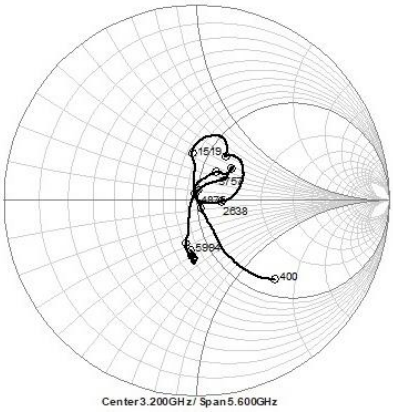

Fig. 10 Smith chart

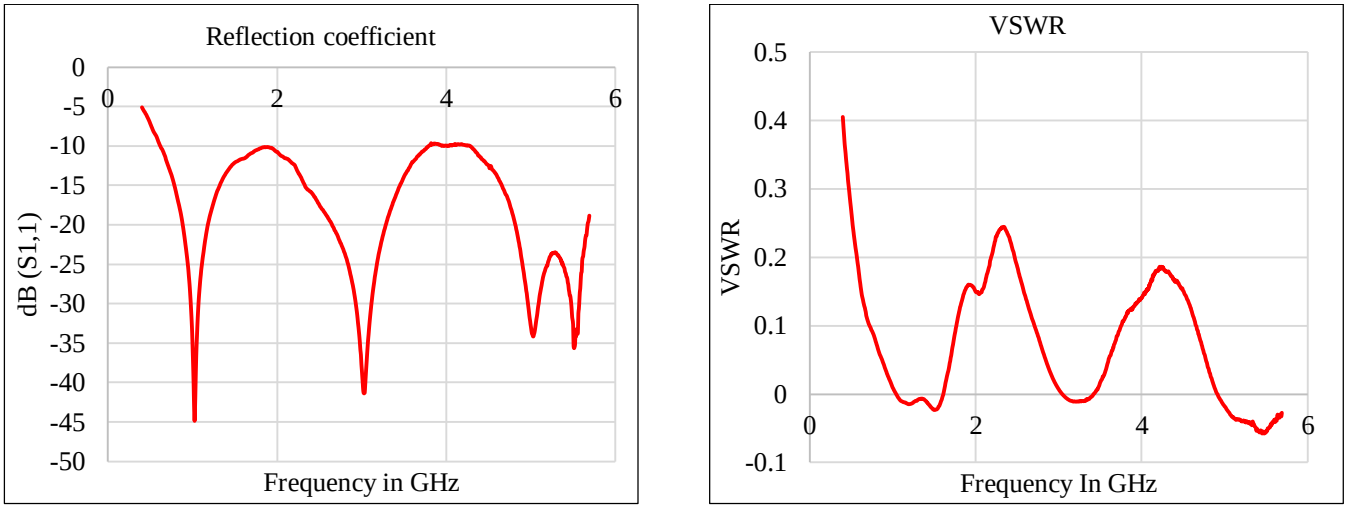

Fig. 11 Smith chart, reflection coefficient, VSWR of fabricated antenna tested on MegiQ VNA0460e

Figure 11 Fabricated Antenna tested result on MegiQ 0460e. In MegiQ, VNA0460e refers to a model of RF equipment produced by MegiQ, a company known for making tools for antenna development and RF signal testing. This particular model is likely part of a Vector Network Analyzer (VNA) series that MegiQ offers, designated for testing and measuring the performance of antennas, cables, and other RF components. The '0460e' model would typically cover a frequency range from 0.4 GHz to 6 GHz, which encompasses many communication bands, including cellular, WiFi, Industrial, Scientific, and Medical (ISM) Band Applications. Featuring a full bi-directional capability, the MegiQ VNA0460e is a 2½-port Vector Network Analyzer that connects to a computer through a USB port. The device is equipped with specialized VNA Software that comes with an integrated Match Circuit Calculator. This tool enables the calculation and real-time simulation of matching circuits derived from network measurements.

Table 4. Analyses of antenna simulated results by using HFSS and measured by using MegiQ 0460e

Sl. No.	Parameter	Frequency (GHz)	VSWR	S11 in dB	Impedance (Ω)
1	Antenna Simulated Results by Using HFSS	2.75, 3.29, 4.86	1.93, 1.24, 1.94	-9.94, -19.16, -9.9	50
2	Antenna Measured Results by Using MegiQ 0460e	2.75, 3.29, 4.86	0.09, -0.01, 0.014	-22.31, -19.55, -22.73	50

Table 5. Comparison between proposed antenna designs with other literature reported

Year	Author	Design	Key Features	Frequency	Notable Performance	Application	Observations
2020	Bhaldar et al.	Wi-Fi Antenna using Denim	Microstrip textile antenna, denim substrate	2.45 GHz	-15.76 dB return loss, 8.05 directivity	Wi-Fi communication	Utilizes common material for substantial bandwidth and performance
2018	Carlos et al.	On-body Antenna & Snap-on Button Design	On-body antenna design, snap-on button	2.45 GHz ISM band	-18 dB to -25 dB return loss	Wireless communication integrated into clothing	Seamless integration into wearable technology
2018	Pranita Manish et al.	Comparative Analysis of Textile Antennas	Different fabric substrates	2.45 GHz	Varied return loss performance	Wearable applications	Material selection's impact on antenna functionality
2014	Sweety Purohit et al.	SAR Study with Jeans Material Antenna	Jeans material as a dielectric substrate	Not specified	Compliant with SAR safety limits	Wearable technology	Balance between communication effectiveness and health standards
2017	Jiahao Zhang et al.	Miniature Feeding Network for Aperture-Coupled Antennas	Various aperture shapes for antennas	2.4 GHz to 2.483 GHz	Enhanced gain and performance	ISM band applications	Exploration of physical configuration effects on performance
2020	Sandeep Singh Sran et al.	Wearable Fractal Antenna	Fractal antenna design	2.53GHz, 4.9GHz, 7.6GHz	Increased gain and bandwidth at resonance	S, C, X band applications	Design for wideband, high-gain performance
Proposed Work		Moon-shaped microstrip patch antenna with a defected ground structure (DGS)	Jeans material as a dielectric substrate for wearable technology applications.	2.75 GHz, 3.29 GHz, 4.86 GHz	-19.16 dB, Compliant with SAR safety limits	Wi-Fi, Bluetooth, and potential 5G applications.	Compactness with high-performance bandwidth requirements for wearable devices in wireless communication

5. Conclusion

This research paper has introduced a novel moon-shaped microstrip antenna design with a defective ground structure tailored for wearable technology applications. The antenna showcases a significant enhancement in bandwidth and performance, attributed to its innovative design features, including a coplanar waveguide feed and a unique ground plane configuration.

The simulation and experimental results confirm the antenna's operational efficacy across a range of frequencies suitable for Wi-Fi, Bluetooth, and potentially GPS applications, making it a versatile component for the next generation of wearable devices. This multifunctionality is particularly valuable in wearable devices that need to maintain connectivity across different communication standards while being close to the human body. The utilization of textile materials for the substrate posits the antenna as a viable solution for seamless incorporation into everyday wearable items, addressing both aesthetic and functional needs without sacrificing performance. The antenna's design not only meets the technical requirements of modern wireless communication systems but also addresses the aesthetic and functional needs of wearable devices. It represents a blend of electrical engineering, material science, and design innovation, paving the way for more user-friendly and integrated wearable technologies. Future work will focus on further optimizing the design for specific applications, exploring the use of different materials for enhanced flexibility and durability, and expanding the antenna's capability to cover additional communication bands.

The graphical results derived from the MegiQ VNA0460e and HFSS simulations substantiate the antenna's capability to operate across a wide frequency range while maintaining high gain, a pivotal requirement for 5G networks. The reflection coefficient plots provide a clear indication that the antenna exhibits resonant behavior at multiple frequencies, demonstrating its wideband characteristics.

This is further emphasized by the Smith Chart, where the trace circles the center point at multiple frequencies, indicating that the antenna maintains its impedance match over a wide frequency range. The dimensions and shape of the modified ground plane are critical in achieving the desired electrical characteristics and in ensuring that the antenna can support the wide frequency range necessary for 5G applications.

References

[1] Jeong-Hun Park, and Moon-Que Lee, "Wide E-Plane Beamwidth Microstrip Patch Antenna Using H-Shaped Gap-Coupling with Three Parasitic Patches for the K-Band," *International Journal of RF and Microwave Computer-Aided Engineering*, vol. 2023, pp. 1-15, 2023. [CrossRef] [Google Scholar] [Publisher Link]

[2] T.O. Olawoye, and P. Kumar, "A High Gain Antenna with DGS for Sub-6 GHz 5G Communications," *Advanced Electromagnetics*, vol. 11, no. 1, pp. 41-50, 2022. [CrossRef] [Google Scholar] [Publisher Link]

[3] Cheon-Bong Moon et al., "Design and Analysis of a Thinned Phased Array Antenna for 5G Wireless Applications," *International Journal of Antennas and Propagation*, vol. 2021, pp. 1-8, 2021. [CrossRef] [Google Scholar] [Publisher Link]

[4] Elham Serria et al., "A Review of Lunar Communications and Antennas: Assessing Performance in the Context of Propagation and Radiation," *Sensors*, vol. 23, no. 24, pp. 1-27, 2023. [CrossRef] [Google Scholar] [Publisher Link]

[5] Anurag Saxena, and Vinod Kumar Singh, "A Moon-Strip Line Antenna for Multi-Band Applications at 5.44 GHz Resonant Frequency," *2018 4th International Conference on Advances in Electrical, Electronics, Information, Communication and Bio-Informatics (AEEICB)*, Chennai, India, pp. 1-3, 2018. [CrossRef] [Google Scholar] [Publisher Link]

[6] B. Rama Sanjeeva Reddy, and A. Amulya Kumar, "Dual Band Circular Polarized Wearable Antenna for Military Applications," *2018 International CET Conference on Control & Communication*, Thiruvananthapuram, India, pp. 220-223, 2018. [CrossRef] [Google Scholar] [Publisher Link]

[7] Nikhil Kumar Singh, Vinod Kumar Singh, and Naresh B., "Textile Antenna for Microwave Wireless power Transmission," *Procedia Computer Science*, vol. 85, pp. 856-861, 2016. [CrossRef] [Google Scholar] [Publisher Link]

[8] Wa'il A. Godaymi Al-Tumah, Raed M. Shaaban, and Akeel Tahir, "Design, Simulation and Measurement of Triple Band Annular Ring Microstrip Antenna Based on Shape of Crescent Moon," *AEU - International Journal of Electronics and Communications*, vol. 117, 2020. [CrossRef] [Google Scholar] [Publisher Link]

[9] Husain Bhaldar et al., "Design of Wearable Multiband Circular Microstrip Textile Antenna for WiFi/WiMAX Communication," *Engineering and Technology Journal*, vol. 6, no. 3, pp. 798-806, 2021. [CrossRef] [Google Scholar] [Publisher Link]

[10] Husain Bhaldar et al., "Design of High Gain Wearable Rectangular Microstrip Textile Antenna for Wireless Application," *International Journal of Innovative Technology and Exploring Engineering*, vol. 9, no. 5, pp. 540-544, 2020. [CrossRef] [Google Scholar] [Publisher Link]

[11] Carlos Mendes, and Custódio Peixeiro, "On-Body Transmission Performance of a Novel Dual-Mode Wearable Microstrip Antenna," *IEEE Transactions on Antennas and Propagation*, vol. 66, no. 9, pp. 4872-4877, 2018. [CrossRef] [Google Scholar] [Publisher Link]

[12] Shengjian Jammy Chen, Damith Chinthana Ranasinghe, and Christophe Fumeaux, "A Robust Snap-On Button Solution for Reconfigurable Wearable Textile Antennas," *IEEE Transactions on Antennas and Propagation*, vol. 66, no. 9, pp. 4541-4551, 2018. [CrossRef] [Google Scholar] [Publisher Link]

[13] Pranita Manish Potey, and Kushal Tuckley, "Design of Wearable Textile Antenna with Various Substrate and Investigation on Fabric Selection," *2018 3rd International Conference on Microwave and Photonics (ICMAP)*, Dhanbad, India, pp. 1-2, 2018. [CrossRef] [Google Scholar] [Publisher Link]

[14] Sweety Purohit, and Falguni Raval, "Wearable Textile Patch Antenna Using Jeans as Substrate at 2.45 GHz," *International Journal of Engineering Research & Technology*, vol. 3, no. 5, pp. 2456-2460, 2014. [Google Scholar] [Publisher Link]

[15] Jiao Zhang, Sen Yan, and Guy A.E. Vandenbosch, "Miniature Feeding Network for Aperture-Coupled Wearable Antennas," *IEEE Transactions on Antennas and Propagation*, vol. 65, no. 5, pp. 2650-2654, 2017. [CrossRef] [Google Scholar] [Publisher Link]

[16] Sandeep Singh Sran, and Jagtar Singh Sivia, "ANN and IFS Based Wearable Hybrid Fractal Antenna with DGS for S, C, and X Band Application," *AEU - International Journal of Electronics and Communications*, vol. 127, 2020. [CrossRef] [Google Scholar] [Publisher Link]

[17] R. Dewan et al., "Crescent Moon-Shaped Artificial Magnetic Conductor Ground Plane for Patch Antenna Application," *2013 IEEE Symposium on Wireless Technology & Applications (ISWTA)*, Kuching, Malaysia, pp. 254-258, 2013. [CrossRef] [Google Scholar] [Publisher Link]

[18] Karteek Viswanadha, and Nallanthighal Srinivasa Raghava, "Design and Analysis of a Multi-Band Flower Shaped Patch Antenna for WLAN/WiMAX/ISM Band Applications," *Wireless Personal Communications*, vol. 112, pp. 863-887, 2020. [CrossRef] [Google Scholar] [Publisher Link]

[19] Vinod H. Patil et al., "A Testbed Design of Spectrum Management in Cognitive Radio Network Using NI USRP and LabVIEW," *International Journal of Innovative Technology and Exploring Engineering*, 2019, vol. 8, no. 9S2, pp. 257-262, 2019. [CrossRef] [Google Scholar] [Publisher Link]

[20] Amir Hossein Haghparast, and Gholamreza Dadashzadeh, "A Dual Band Polygon Shaped CPW-Fed Planar Monopole Antenna with Circular Polarization and Isolation Enhancement for MIMO Applications," *2015 9th European Conference on Antennas and Propagation (EuCAP)*, Lisbon, Portugal, pp. 1-4, 2015. [Google Scholar] [Publisher Link]

[21] Renuka Wadhwa, and Sukhdeep Kaur, "Moon Shape Microstrip Patch Antenna with Stair Case Ground," *International Journal on Recent and Innovation Trends in Computing and Communication*, vol. 3, no. 6, pp. 4209-4213, 2015. [Google Scholar] [Publisher Link]

[22] Patrick Danuor, Jung-Ick Moon, and Young-Bae Jung, "High-Gain Printed Monopole Antenna with Dual-Band Characteristics Using FSS-Loading and Top-Hat Structure," *Scientific Reports*, vol. 13, pp. 1-12, 2023. [CrossRef] [Google Scholar] [Publisher Link]

[23] Roshanak Elyassi, and Gholamreza Moradi, "Flexible and Moon-Shaped Slot UWB Implantable Antenna Design for Head Implants," *International Journal of Microwave and Wireless Technologies*, vol. 9, no. 8, pp. 1559-1567, 2017. [CrossRef] [Google Scholar] [Publisher Link]

[24] Kang Ding, Yong-Xin Guo, and Cheng Gao, "CPW-Fed Wideband Circularly Polarized Printed Monopole Antenna with Open Loop and Asymmetric Ground Plane," *IEEE Antennas and Wireless Propagation Letters*, vol. 16, pp. 833-836, 2016. [CrossRef] [Google Scholar] [Publisher Link]

[25] Qiang Chen et al., "Broadband CPW-Fed Circularly Polarized Planar Monopole Antenna with Inverted-L Strip and Asymmetric Ground Plane for WLAN Application," *Progress in Electromagnetics Research C*, vol. 74, pp. 91-100, 2017. [CrossRef] [Google Scholar] [Publisher Link]

[26] Benyang Hu, Nasimuddin, and Zhongxiang Shen, "Broadband Circularly Polarized Moon-Shaped Monopole Antenna," *Microwave and Optical Technology Letters*, vol. 57, no. 5, pp. 1135-1139, 2015. [CrossRef] [Google Scholar] [Publisher Link]

[27] Benyang Hu, Nasimuddin, and Zhongxiang Shen, "Moon-Shaped Printed Monopole Antenna for Wideband Circularly Polarized Radiation," *2013 IEEE-APS Topical Conference on Antennas and Propagation in Wireless Communications (APWC)*, Turin, Italy, pp. 825-827, 2013. [CrossRef] [Google Scholar] [Publisher Link]

[28] Jingli Guo, Yanlin Zou, and Chao Liu, "Compact Broadband Crescent Moon-Shape Patch-Pair Antenna," *IEEE Antennas and Wireless Propagation Letters*, vol. 10, pp. 435-437, 2011. [CrossRef] [Google Scholar] [Publisher Link]

[29] Wa'il A. Godaymi Al-Tumah, Raed M. Shaaban, and Alistair P. Duffy, "Design, Simulation, and Fabrication of a Double Annular Ring Microstrip Antenna Based on Gaps with Multiband Feature," *Engineering Science and Technology, an International Journal*, vol. 29, pp. 1-10, 2022. [CrossRef] [Google Scholar] [Publisher Link]

[30] Waleed Shihzad et al., "Design and Analysis of Dual-Band High-Gain THz Antenna Array for THz Space Applications," *Applied Sciences*, vol. 12, no. 18, pp. 1-20, 2022. [CrossRef] [Google Scholar] [Publisher Link]

[31] Anveshkumar Nella, and A.S. Gandhi, "Moon Slotted Circular Planar Monopole UWB Antenna Design and Analysis," *2017 International Conference on Advances in Computing, Communications and Informatics (ICACCI)*, Udupi, India, pp. 595-600, 2017. [CrossRef] [Google Scholar] [Publisher Link]

[32] Boya Satyanarayana, and S.N. Mulgi, "Parametric Analysis of Planar Circular Monopole Antenna for UWB Communication Systems," *International Journal of Advanced Research in Electrical, Electronics and Instrumentation Engineering*, vol. 3, no. 9, pp. 12068-12074, 2014. [CrossRef] [Google Scholar] [Publisher Link]

[33] C.Y.D. Sim et al., "Broadband Circularly Polarized Antenna with Moon-Shaped Parasitic Element," *International Journal of RF and Microwave Computer-Aided Engineering*, vol. 26, no. 5, pp. 387-395, 2016. [CrossRef] [Google Scholar] [Publisher Link]

[34] Seyed Mohsen Hosseini Varkiani, and Majid Afsahi, "Compact and Ultra-Wideband CPW Fed Square Slot Antenna for Wearable Applications," *AEU - International Journal of Electronics and Communications*, vol. 106, pp. 108-115, 2019. [CrossRef] [Google Scholar] [Publisher Link]